



Multiyear surface waves dataset from the subsurface "DeepLev" Eastern Levantine moored station

Nir Haim¹, Vika Grigorieva¹, Yaron Toledo¹, Rotem Soffer¹, Boaz Mayzel¹, Timor Katz², Ronen Alkalay^{2,3}, Eli Biton², Ayah Lazar², Hezi Gildor⁴, Ilana Berman-Frank⁵, Yishai Weinstein³, and Barak Herut²

¹School of Mechanical Engineering, Faculty of Engineering, Tel Aviv University, Tel-Aviv, 6997801, Israel

²Israel Oceanographic & Limnological Research, Tel Shikmona, Haifa, 31080, Israel

³Department of Geography and Environment, Bar-Ilan University, Ramat-Gan, 52900, Israel

⁴Institute of Earth Sciences, Hebrew University, Jerusalem, 91904, Israel

⁵Dept. of Marine Biology, Leon H. Charney School of Marine Sciences, University of Haifa, Haifa, 3498838, Israel

Correspondence: Yaron Toledo (toledo@tauex.tau.ac.il)

Abstract.

Processed and analyzed sea surface wave characteristics derived from an up-looking Acoustic Doppler Current Profiler (ADCP) for the period 2016-2022 are presented as a dataset. The collected data include full two-dimensional wave fields along with computed bulk parameters, such as wave heights, periods, and directions of propagation. The ADCP was mounted on the submerged Deep Levantine mooring station located 50 km off the Israeli coast to the west of Haifa (bottom depth ~1470m). It meets the need for accurate and reliable in situ measurements in the Eastern Mediterranean Sea, as the area significantly lacks wave data compare to other Mediterranean sub-basins. The developed long term timeseries of wave parameters allow for monitoring and analysis of the region's wave climate, as well as a deeper understanding of wind-wave generation mechanisms.

1 Introduction

Monitoring ocean waves is crucial for support in making informed decisions related to the development, protection, and management of the marine and coastal environments. Accurate and regular wave measurements are also of great importance in numerous research fields, for example in studying air-sea and wave-current interactions (Wolf and Prandle, 1999), analysing climate changes or investigating the effects of waves dispersion of particles and oil slicks in the water (Fanelop and Waldman, 1972; Sobey and Barker, 1997; Röhrs et al., 2012). Furthermore, the renewable energy sectors seek to harness ocean waves for power generation, and precise wave monitoring is essential for optimizing the design and operation of wave energy converters (Lira-Loarca et al., 2021). There are increasing efforts to gather information of the sea state in the Mediterranean sea (Tintoré et al., 2019), still the Levantine basin is comparably lacking in observations (Toomey et al., 2022).

To meet these needs, the Deep Levantine (DeepLev) station was moored on November 2016 about 50 km off-shore Haifa, Israel, at 33°00'N, 34°30'E. It was the first of its kind, deep ocean moored marine research station in the East Levantine Basin (ELB). The station has been serving as a platform for a large number of state-of-the-art measuring instruments. The mooring cable extended from the seabed at depth of approximately 1470 m up to a subsurface buoy (at a nominal depth of ~ 30 m)



carrying an up-looking Acoustic Doppler Current Profiler (ADCP). Katz et al. (2020) gives a full description of the mooring system and carried equipment. In general, instruments for waves measurements are deployed at shallow and intermediate waters (20-40 m depth). A quite understandable practice considering the added complexity and hence increased costs involved in deep sea surveys. Nonetheless, long-term observations at deep waters are valuable for continuous monitoring of sea state. Moreover, avoiding the presence of nearshore bathymetry changes or shore reflections allows for a better accuracy evaluation of wave models and satellite measurements.

In this study, for the first time, a multi-year open-source dataset of wave spectra and derived wave characteristics (i.e. heights, periods, directions) has been developed from DeepLev station measurements for the period 2016-2022. The paper is organized as follows. Section 2 is dedicated to a general description of the measuring instrument, its operation principles and evaluation of wave information. Section 3 deepens into the collected data, expanding about the processing, issues that emerged and their implications on quality. Conclusive Section 4 finalizes the paper by listing the main results and perspectives of deep sea measurements and wave monitoring in the ELB.

2 Methodology

2.1 Acoustic Doppler current profiler wave measurements

As it was mentioned above, the DeepLev station is a multi-functional platform equipped by numerous measuring systems for monitoring the sea state and marine environment. Throughout the whole campaign (2016-2022) the Norteks' Signature-500 ADCP was used to measure surface wave parameters thus the derived data are consistent and homogeneous (figure 1 shows the subsurface buoy and ADCP mounted on it). The practice of combining of the Nortek's ADCPs and subsurface buoys was found to be successful (Pedersen et al., 2007), though with possible minor data artifacts due to the buoy's wave induced movement. Compared to Pedersen et al. (2007), in this study the subsurface buoy was deeper therefore expected to be less responsive to surface waves' motion.

The Signature-500 has three types of sensors: a pressure sensor, four slanted acoustic beams, and a single vertical acoustic beam—which gives it an advantage over other types of ADCPs allowing for different wave field evaluation approaches to be applied. The first method is solely relied on the slanted acoustic beams. The transmitted signals and received Doppler shifted back-scatter (Rowe and Young, 1979; McDaniel and Gorman, 1982) enable to estimate wave characteristics, including the directional wave spectrum, $S^{vel}(f, \theta)$ from the induced orbital velocities near the surface (Bowden and White, 1966). The main limit of the "velocity-based" (hereinafter, VEL) method is its sensitivity to installation depth. In deep installations the horizontal spacing between the beams increases beyond the solution's validity. Within the DeepLev's settings, the theoretical upper cut-off at 30 meters depth is 3.85 sec for directional parameters and 1.15 sec for non-directional.

The second method uses the vertically oriented fifth beam for acoustic surface tracking (AST). The measurement of the surface elevation can be directly represented as a one dimensional spectrum $S^{ast}(f)$. Here, even short waves which cannot be detected by the slanted beams' array are visible to the AST. Pedersen et al. (2007) offered a way to expand the surface tracking information into directional spectrum, $S^{su}(f, \theta)$, by combining correlated velocity measurements. This method is



55 known as "SUV" suggesting the combination of surface tracking (S) with horizontal velocities (UV). The name references a
 third method, the established "PUV" technique (Panicker and Borgman, 1974) which applies similar calculations with pressure
 observations instead. But in this study the installation is too deep to measure pressure fluctuations made by the surface wave
 field.

60 Prior to each deployment the device's operation mode was configured balancing between the expected duration in the sea
 and available battery capacity. Table 1 summarizes details of the deployments including the configuration of the experiment,
 its duration, cycle intervals, and sampling frequency. Most of the time, the ADCP was configured to operate with a sampling
 frequency of 2 Hz, with the exception of the fourth deployment when the sampling frequency was 4Hz. The cycle intervals are
 regulated by two different modes of Signature-500 ("Burst" and "Continuous"). When set to "Burst mode", the device worked
 at intervals and collected only 2048 continuous samples withing a cycle (equivalent to about 17 min when using 2Hz). The
 65 intervals between cycles were also predetermined and are listed in Table 1. The third and fourth deployments measured in
 "Continuous" mode without any pauses. For the purpose of consistency, their measurements were analyzed to provide 17 min
 averages as the rest of the deployments.

2.2 Surface waves averages and directional properties extraction

70 The first stage of data processing was performed by Nortek's "Ocean Contour" Software, which synthesizes the primary binary
 files into wave information. The simplest type of analysis provided is by directly identifying individual waves in the surface
 elevation timeseries, $\eta(t)$. Then, wave characteristics are summarized into the maximal measured wave height H_{max} and period
 T_{max} , the mean height H_{mean} , mean zero-crossing T_z , averages over heights and periods of the highest 1/3 of the waves, H_3
 and T_3 , and over the highest 1/10 of the waves, H_{10} and T_{10} .

75 Additionally, the timeseries signals are converted using fast Fourier transform into spectral variance density function $S(f)$
 that indicates how much of the surface wave elevation variance is contained at the specific frequencies f . This spectral repre-
 sentation highlights the peak frequency f_p , the most energetic frequency inversely related to the peak period T_p . Other bulk
 parameters are calculated through the energy-spectrum's moments (Tucker, 1993), with the moment of order n defined as

$$m_n = \int_0^{\infty} f^n S(f) df, \quad (1)$$

80 where $S(f)$ is the directional-averaged density spectrum. The parameters calculated from the spectral moments are the signifi-
 cant wave height $H_{m0} = 4\sqrt{m_0}$, which is considered comparable to H_3 , the mean wave period $T_{m02} = \sqrt{\frac{m_0}{m_2}}$, and the energy
 period $T_{energy} = m_{-1}/m_0$, a weighted mean period based on the spectral density which is useful in estimating wave energy
 potential. For directional data, the mean wave direction per wave frequency, $\theta_m(f)$, is obtained from the first harmonic Fourier
 coefficients of the power density spectrum function $S(f, \theta)$ and the corresponding Fourier coefficients $a_n(f)$, $b_n(f)$ as follows

$$85 \quad \theta_m(f) = \arctan \frac{b_1(f)}{a_1(f)}, \quad a_n(f) = \frac{1}{S(f)} \int_0^{2\pi} S(f, \theta) \cos n\theta d\theta, \quad b_n(f) = \frac{1}{S(f)} \int_0^{2\pi} S(f, \theta) \sin n\theta d\theta. \quad (2)$$



The reported mean wave direction θ_m is a weighted average of $\theta_m(f)$ in each frequency bin according to its energy. The peak direction θ_p is the peak of the spread function constructed employing Fourier coefficients of all available harmonics ($n=2$) for the peak frequency. Both estimations are expressed here in meteorological conventions, i.e. the specified direction is the direction which the waves are coming from.

90 The applied methodology provide a complete set of standard wave characterises and allow to compare the results with models, satellites, buoys, and visual wave observations on equal terms.

3 Results

The developed dataset presented in this paper includes processed, corrected and analyzed measurements from eight ADCP deployments for the period 2016-2022. In order to save maximum wave information we stored all measurements passed the
95 original Norteks' software quality control. However, the data were complemented by quality indexes based on detailed analysis of observations.

3.1 Data integrity and correction

Overall, the observations presented here cover a period equivalent to 4.9 consecutive years, between 14-Nov-2016 and 30-Aug-2022. As to the writing of this paper, the DeepLev operation is still ongoing, carrying the ninth deployment of the wave
100 monitoring ADCP. Table 2 describes the data obtained from each deployment along with assigned quality indexes. Predictably, the majority of observations are of good quality and provide the full set of wave characteristics including directional information. A recent comparison of the DeepLev's first deployment Soffer et al. (2020) and parallel experiment with bottom mounted ADCP also indicates the quality and reliability of Signature-500 measurements. However, we have faced several challenges during data processing and analysis. Some of them were resolved and others yet to be explained.

105 The initial challenge we encountered was a considerable variability in the percentages of "Ambiguous" data indicating the inability of the system to determine a local maximum of the wave energy spectra. The situation occurs more frequently with lower ambiguity frequency resulted of higher nominal depth of the buoy carrying the ADCP. When installing a moored station with 1470 m long cable, it was difficult to ensure the depth of the sub-surface buoy. In practice, the nominal depths varied by 12 m, therefore some deployments retrieved higher percentages of directional data than others. The analysis showed that for
110 the specific wave characteristics securing the instrument at 30 m bellow the sea surface would add another valid 10% of data to the gathered wave directional information.

Only a small portion of the measurements were found to be unreasonable or completely missing. Occasionally, if there is a problem with returning bursts or if the device has trouble detecting the surface it will lead to missing points after processing. Unfortunately, two of the deployments (the fourth and the eighth) had issues resulting in abnormal data loss. During the fourth
115 deployment, it seems like something obstructed the device as evidenced by notable deviations between the measured distance and pressure. A relatively short timeseries of the eighth deployment stem from an unexpected malfunction of the memory card.



Another problem was addressed after the initial processing. In both, the second and third deployments, the instrument returned without the ordinary temperature observations. Normally, this information is used to evaluate the water's sound velocity (SV) which is necessary to translate the return time of a burst to distance. As a consequence of the fault, all subsequent calculations were carried out with a SV value of 1300 m/sec. This default values is lower by about 20% than the expected ones and led to similar inaccuracies in computed length scales. To correct these values, the missing temperatures were replaced with records by a secondary temperature sensor attached to the pressure sensor. Using these data, the SV was recalculated with the Gibbs-SeaWater (GSW) Oceanographic Toolbox (McDougall and Barker, 2011). Then the calculated parameters were adjusted according to the ratio between the new SV and the original ones. The correction was easily confirmed by comparing the adjusted distance from the AST measurement and the pressures. In this regard, one should consider that the SV used for calculations is constant even if the water column is strongly stratified. As it happened during the local summers when according to the temperature measurements the thermocline was located above the ADCP. Then, the assumption that the measured values fitted the entire water column turns out to be inaccurate. In such a case the calculations are based on a temperature measured below the thermocline while the water column between the device and the surface are likely $8^{\circ}\text{C} - 10^{\circ}\text{C}$ warmer. As a result, the uncertainties in SV and wave height estimates could reach 2 – 3%.

Lastly, observing waves from a submerged subsurface buoy adds complexity since the measurements are coming out from a moving platform. The processing software uses records from the tilt sensors for corrections. But, to get a good reading from the AST sensor the tilt must be lower than 10° . With specified DeepLev station mooring settings, there were no instances of tilt too high, the maximum registered was about 8° .

3.2 Data review

The developed dataset represents an open source of surface wave characteristics derived from ADCP measurements (<https://doi.org/10.17882/96904>). The number of files corresponds to the number of deployments which simplify the selection of the timeseries of interest. The used NetCDF4 format guarantees easy access and eliminates occasional reading errors. Each file contains the time varying spectra $S^{ast}(f)$, $S^{vel}(f, \theta)$ and $S^{suw}(f, \theta)$. In addition, it includes unified arrays of the aforementioned statistical wave parameters with preference to values derived from $S^{suw}(f, \theta)$. The frequency range for wave spectra is 0.02-0.45 Hz with the step of 0.005 Hz. The upper limit was adopted as preliminary data processing had showed that the highest resolved frequency was 0.445 Hz which corresponds to a minimal distance from the sea surface of 27.8 m. A few isolated events led the ADCP to experience deepening of over 10 m. The maximal recorded depth was 54 m on Mar 20th 2022, thus lowering the frequency ambiguity limit to 0.195 Hz. A full description of the files with detailed specification of each wave parameter is available in the appendix.

Figure 3 shows a timeseries of H_{m0} and T_p reconstructed by two methods (VEL and AST) for a short period out of the 3rd deployment. This time frame includes the highest observed waves event of the entire campaign when H_{m0} reached 8 m. Apparently, when the surface waves are high and long there is a good agreement between the two methods. The preference of using the AST approach is eminent in young waves conditions (fig 3b). When it comes to directional spectra, the ability of ADCP is limited in very rough sea state, so the example for retrieved spectra is taken after the peak of the event (Figure 4).



Both methods demonstrate a consistency in directional distributions. The incorporation of the AST in the SUV method adjusts the intensities and energy distribution between frequency bins.

Figure 2 displays the distributions of H_{m0} , H_{max} , T_p and T_{m02} among all the data collected. Though there are gaps between deployments, all months were sampled fairly evenly so the results are not expected to be strongly biased. The most probable wave statistics at the DeepLev location have a significant wave height between 0.5 m and 1 m and a peak period of 5-6 sec. Moreover, at least half the time the H_{m0} is over 0.8 m and finding it measuring up to 2.5 m with H_{max} of 4 m is common.

4 Summary and Conclusion

For the first time ever wind wave characteristics have been assembled together after multistage data processing, correction, and analysis in the deep Levantine Sea. The developed dataset derived from an Acoustic Doppler Current Profiler for the period 2016-2022 is a part of the comprehensive DeepLev project which involves monitoring of physical, biological and chemical properties in the Levantine basin off the Israeli shore. The analyzed data constitute a timeseries of full two-dimensional wave fields, calculated by two methods utilizing wave orbital velocities and surface tracking, along with conventional statistical parameters: wave heights, periods, and directions of propagation.

Such a valuable add-on to the exploring of the Levantine Sea is of importance considering the deficiency of observations compared to other sub-basins of the Mediterranean Sea. Reliable continuous timeseries of various surface wave characteristics allow getting additional insight to mechanisms of wave generation, growing, and decay. Moreover, the collected data can be effectively used for monitoring wave climate changes on seasonal and long term scales as well as for evaluation of extreme wave characteristics in the Eastern Mediterranean. Besides scientific findings, this experiment also have brought valuable insights on long exploitation of the ADCP Nortek “Signature 500” in deep waters.

To finalize the paper, we would like to stress the value and importance of a unique five year dataset of wave characteristics in the deep waters of the Eastern Mediterranean basin for sea state monitoring.

Data availability.

Described data are freely available through SEANOE (SEA scieNtific Open data Edition) open scientific data repository: <https://doi.org/10.17882/96904> (Nir et al., 2022).



175 *Author contributions.* NH managed processing and organization of data, NH, VG, and YT wrote the manuscript, analysed, evaluated and visualized the processed data. YT, RS and BM maintained the Signature 500 instrument and its operation. The authors TK, RA, EB, AL, HG, IB-F, YW and BH contributed via their labor in the long-term ongoing DeepLev project, its maintenance, operation and management. Funds were raised by IB-F, IW, BH and YT

Competing interests. none

180 *Acknowledgements.* This research was supported by the ISRAEL SCIENCE FOUNDATION [grant No. 25/2014 (IW); and 1940/14 and 1601/20 (YT)] in frame of the used equipment and the student grants. We are grateful to the Council for Higher Education in Israel and the Mediterranean Sea Research Centre of Israel (MERCİ), the Wolfson Foundation, the North American Friends of IOLR and Bar-Ilan University (BIU) for funding the construction and maintenance of DeepLev. This project was supported by the Israeli Ministries of Energy and Environmental Protection under the framework of the National Monitoring Program for Israeli Mediterranean Waters. We would like
185 to show our appreciations to the IOLR electronic, sea operations and marine physical departments for invaluable help with facilities and technical operations in establishing and running the DeepLev station, the captain and crew of R/V Bat-Galim, and the engineers of the machine shop at BIU for their help in the buildup of mooring.



References

- Bowden, K. and White, R.: Measurements of the orbital velocities of sea waves and their use in determining the directional spectrum, *Geophysical Journal International*, 12, 33–54, 1966.
- Fannelop, T. K. and Waldman, G. D.: Dynamics of oil slicks, *AIAA Journal*, 10, 506–510, 1972.
- Katz, T., Weinstein, Y., Alkalay, R., Biton, E., Toledo, Y., Lazar, A., Zlatkin, O., Soffer, R., Rahav, E., Sisma-Ventura, G., et al.: The first deep-sea mooring station in the eastern Levantine basin (DeepLev), outline and insights into regional sedimentological processes, *Deep Sea Research Part II: Topical Studies in Oceanography*, 171, 104 663, 2020.
- 195 Lira-Loarca, A., Ferrari, F., Mazzino, A., and Besio, G.: Future wind and wave energy resources and exploitability in the Mediterranean Sea by 2100, *Applied Energy*, 302, 117 492, 2021.
- McDaniel, S. T. and Gorman, A. D.: Acoustic and radar sea surface backscatter, *Journal of Geophysical Research: Oceans*, 87, 4127–4136, 1982.
- McDougall, T. J. and Barker, P. M.: Getting started with TEOS-10 and the Gibbs Seawater (GSW) oceanographic toolbox, *Scor/lapso WG*, 200 127, 1–28, 2011.
- Nir, H., Yaron, T., Boaz, M., Vika, G., Rotem, S., Timor, K., Ronen, A., Eli, B., Ayah, L., Hezi, G., Ilana, B.-F., Yishai, W., and Barak, H.: Surface waves data from a submerged ADCP in the "DeepLev" Eastern Levantine station, <https://doi.org/10.17882/96904>, "SEANOE", 2022.
- Panicker, N. N. and Borgman, L. E.: Enhancement of directional wave spectrum estimates, in: *Coastal Engineering 1974*, pp. 258–279, 1974.
- 205 Pedersen, T., Siegel, E., and Wood, J.: Directional wave measurements from a subsurface buoy with an acoustic wave and current profiler (AWAC), in: *OCEANS 2007*, pp. 1–10, IEEE, 2007.
- Röhrs, J., Christensen, K. H., Hole, L. R., Broström, G., Drivdal, M., and Sundby, S.: Observation-based evaluation of surface wave effects on currents and trajectory forecasts, *Ocean Dynamics*, 62, 1519–1533, 2012.
- Rowe, F. and Young, J.: An ocean current profiler using Doppler sonar, in: *OCEANS'79*, pp. 292–297, IEEE, 1979.
- 210 Sobey, R. J. and Barker, C. H.: Wave-driven transport of surface oil, *Journal of Coastal Research*, pp. 490–496, 1997.
- Soffer, R., Vrecica, T., Kit, E., and Toledo, Y.: Observations, modeling, and inter-comparison of waves from deep to intermediate waters in the East Mediterranean basin, *Deep Sea Research Part II: Topical Studies in Oceanography*, 171, 104 646, 2020.
- Tintoré, J., Pinardi, N., Álvarez-Fanjul, E., Aguiar, E., Álvarez-Berastegui, D., Bajo, M., Balbin, R., Bozzano, R., Nardelli, B. B., Cardin, V., et al.: Challenges for sustained observing and forecasting systems in the Mediterranean Sea, *Frontiers in Marine Science*, p. 568, 2019.
- 215 Toomey, T., Amores, A., Marcos, M., and Orfila, A.: Coastal sea levels and wind-waves in the Mediterranean Sea since 1950 from a high-resolution ocean reanalysis, *Frontiers in Marine Science*, 9, 991 504, 2022.
- Tucker, M.: Recommended standard for wave data sampling and near-real-time processing, *Ocean engineering*, 20, 459–474, 1993.
- Wolf, J. and Prandle, D.: Some observations of wave–current interaction, *Coastal Engineering*, 37, 471–485, 1999.



#	Deployment start	Deployment end	Duration [days]	Sampling Frequency [Hz]	Interval [min]
1	14-Nov-2016	12-May-2017	179	2	120
2	1-Jun-2017	25-Nov-2017	177	2	120
3	4-Dec-2017	28-Apr-2018	145	2	17*
4	31-Jul-2018	28-Mar-2019	240	4	17*
5	13-May-2019	18-Dec-2019	219	2	120
6	18-Feb-2020	16-Sep-2020	211	2	60
7	27-Oct-2020	3-Nov-2021	372	2	60
8	27-Dec-2021	30-Aug-2022	246	2	60

Table 1. Duration for each of the ADCP deployments with measuring configuration: Sampling frequency of sensors and interval of measurements in "Burst" mode. *The measurements were actually in "Continuous" mode but outputs were averaged in 17 min windows.



#	Nominal depth [m]	Time points	Valid [%]	Ambiguous [%]	Unreasonable [%]	Missing [%]
1	39	2153	82.86	15.00	1.90	0.23
2	31	2128	97.70	1.13	1.08	0.09
3	32	12235	88.39	7.61	3.95	0.06
4	28	20240	84.90	1.93	0.89	12.29
5	29	2621	92.79	4.85	2.37	0.00
6	39	5066	82.23	12.34	2.33	3.10
7	37	8921	84.92	12.70	0.91	1.47
8	27	5905	32.35	2.64	1.61	63.40

Table 2. Summary of quality of data collected at each deployment.



Figure 1. The wave measuring instrument, Nortek's "Signature 500", mounted on the top buoy of the "DeepLev" mooring system.

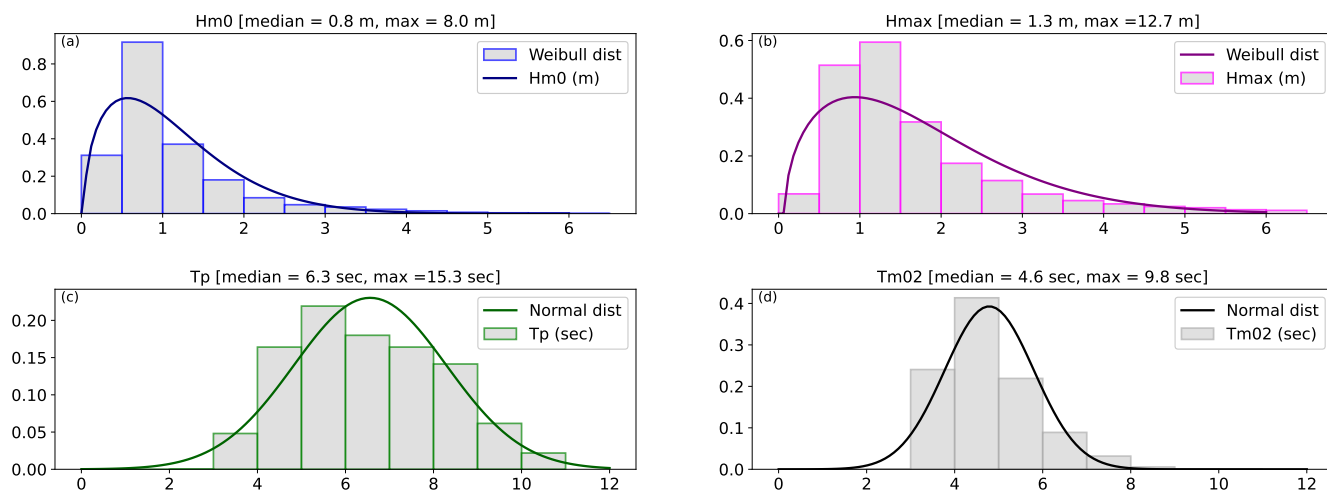


Figure 2. Histograms of combined data from the 8 deployments. a) significant wave heights H_{m0} b) maximal wave heights T_{max} c) peak wave periods T_p d) mean wave periods T_{m02} . Accompanied by approximated probability fits for comparison.

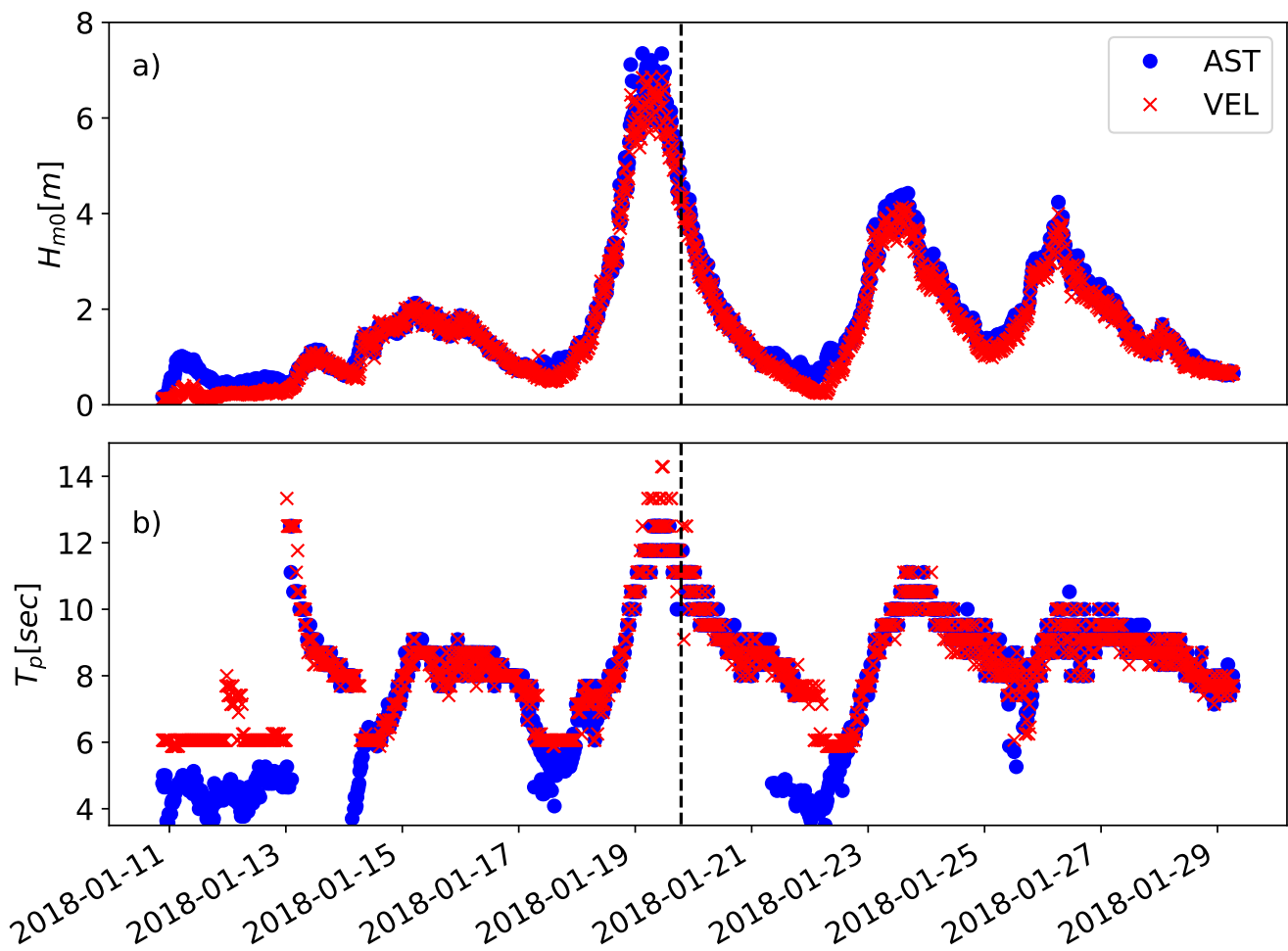


Figure 3. A short timeseries out of the 3rd deployment derived from velocity orbitals (red) or combined with AST (blue)). Shown parameters are a) Significant wave heights and b) peak period. Vertical dashed line marks the date of measurements presented in figure 4

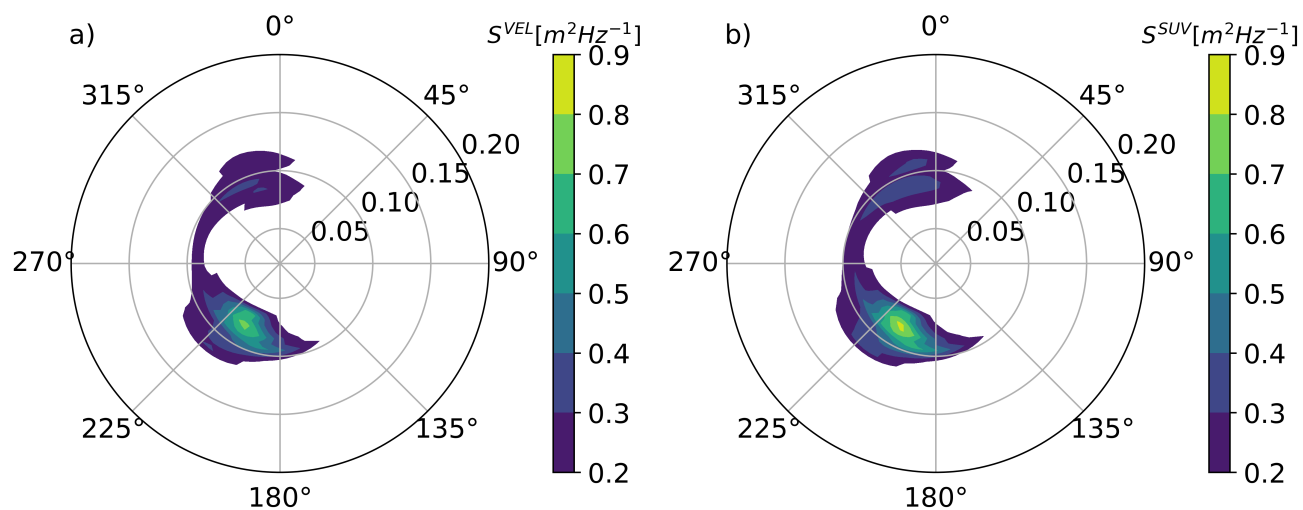


Figure 4. Directional energy density spectra observed on 2018-Jan-19 18:54 processed from a) velocity orbitals, $S^{vel}(\theta, f)$, or b) combined with AST, $S^{suv}(\theta, f)$.



Appendix A

Parameter	Dimensions	Description	Units
Direction	frequency, time	dominant direction of each frequency component	
EnergySpectra	frequency, time	m^2/sec	
FrequencyAmbiguityLimit	time	Cut off frequency for directional estimations	Hz
ASTSpectra Energy	frequency, time	$S^{suv}(\theta, f, t)$ energy density from SUV method	$m^2/Hz/deg$
FullWaveDirectionalSpectra_Energy	time, direction, frequency	$S(\theta, f, t)$ combined energy density from S^{vel} , S^{suv} and S^{puv}	$m^2/Hz/deg$
PressureSpectra_Energy	time, direction, frequency	$S^{puv}(\theta, f, t)$ energy density from PUV method	$m^2/Hz/deg$
VelocitySpectra_Energy	time, direction, frequency	$S^{vel}(\theta, f, t)$ energy density from orbital velocities, VEL method	$m^2/Hz/deg$
WaveSpectra AST	frequency, time	$S^{ast}(f, t)$	m^2/Hz
WaveSpectra Pressure	frequency, time	$S^p(f, t)$	m^2/Hz
WaveSpectra Vel	frequency, time	$S^{vel}(f, t)$	m^2/Hz

Table A1. 1D and 2D spectral energy densities included in the Netcdf files



Parameter	Description	Units
Temperature	averaged temperature	C
Tilt Pitch		degree
Tilt Roll		degree
Heading		degree
Pressure	averaged water column pressure	dbar
Distance	distance from surface measured by vertical acoustic beam	m
Current Direction		degree
Current Speed		m/sec
Direction DirTp	Direction at peak wave period	degree
Direction MeanDir	Mean Direction θ_m	degree
Direction SprTp	Spreading at peak wave period	degree
Height H10	H_{10} : mean height of the 10% largest waves (observed by AST)	m
Height H3	H_3 : mean height of the 33% largest waves (observed by AST)	m
Height Hm0	$H_{m0} = 4\sqrt{m_0}$: spectral significant height	m
Height Hmean	H_{mean} : mean height of the surface waves (observed by AST)	m
Height Hmax	H_{max} : Highest single wave height (observed by AST)	m
Period T10	T_{10} : mean period of the 10% largest waves (observed by AST)	sec
Period T3	T_3 : mean period of the 33% largest waves (observed by AST)	sec
Period Tenergy	$T_{energy} = m_{-1}/m_0$	sec
Period Tm02	$T_{m02} = \sqrt{m_0/m_2}$: spectral mean wave period	sec
Period Tmax	T_{max} : wave period of single largest wave (observed by AST)	sec
Period Tp	$T_p = 1/f_p$ wave period of peak wave frequency	sec
Period Tz	T_z Mean zero-crossing wave period	sec
SpectrumType	origins of values in 1d spectral variables 0: Pressure 1:Velocity 3:AST	
ZeroCrossings	number of zero crossings	
QI	quality index as described in section 3. 1: valid, 2: ambiguous, 3: unreasonable, 4: fault	

Table A2. Timeseries of wave parameters and sensors records included in the Netcdf files.